Supporting Information

Interfacial processing engineering of co-grinding agent for recycling of spent lithium-ion batteries

Jie Ren[a], Zhewen Zhang[e], Zikang Chen[a], Li Wan[b], Kaixiang Shi[a,c], Xiaoyuan Zeng[f], Junhao Li[a,d,*], Quanbing Liu [a,c,*]

[a]Guangzhou Key Laboratory of Clean Transportation Energy Chemistry, Guangdong Provincial Key Laboratory of Plant Resources Biorefinery, School of Chemical Engineering and Light Industry, Guangdong University of Technology, Guangzhou 510006, China

[b]Guangdong Polytechnic of Environmental Protection Engineering, Guangzhou 510655, China

[c]Jieyang Branch of Chemistry and Chemical Engineering Guangdong Laboratory (Rongjiang Laboratory), Jieyang 515200, China

[d]School of Chemistry and Chemical Engineering, South China University of Technology, Guangzhou 510641, China

[e]School of Materials and Energy, Guangdong University of Technology, Guangzhou, 510006, China

[f]National and Local Joint Engineering Laboratory for Lithium-ion Batteries and Materials Preparation Technology, Key Laboratory of Advanced Battery Materials of Yunnan Province, Faculty of Metallurgical and Energy Engineering, Kunming University of Science and Technology, Kunming 650093, China

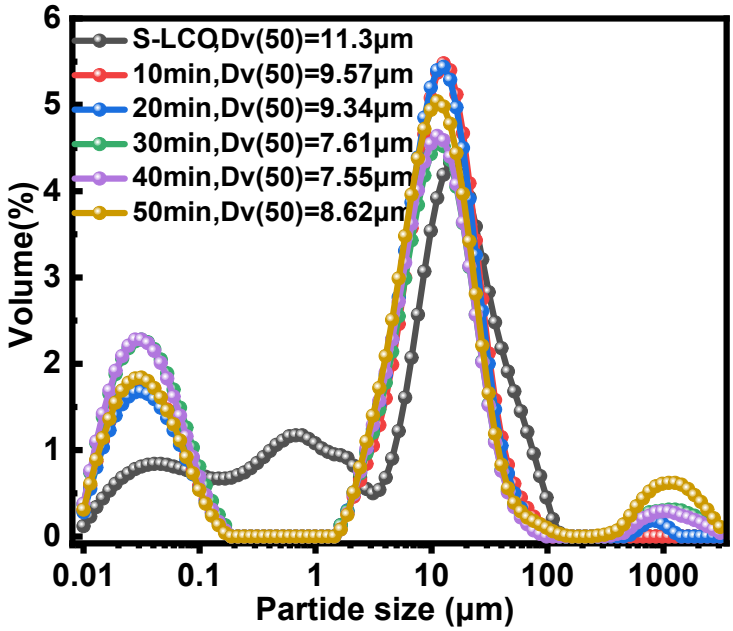

Figure S1. Particle size distribution of S-LCO powders activated at 600 rpm for different milling times.

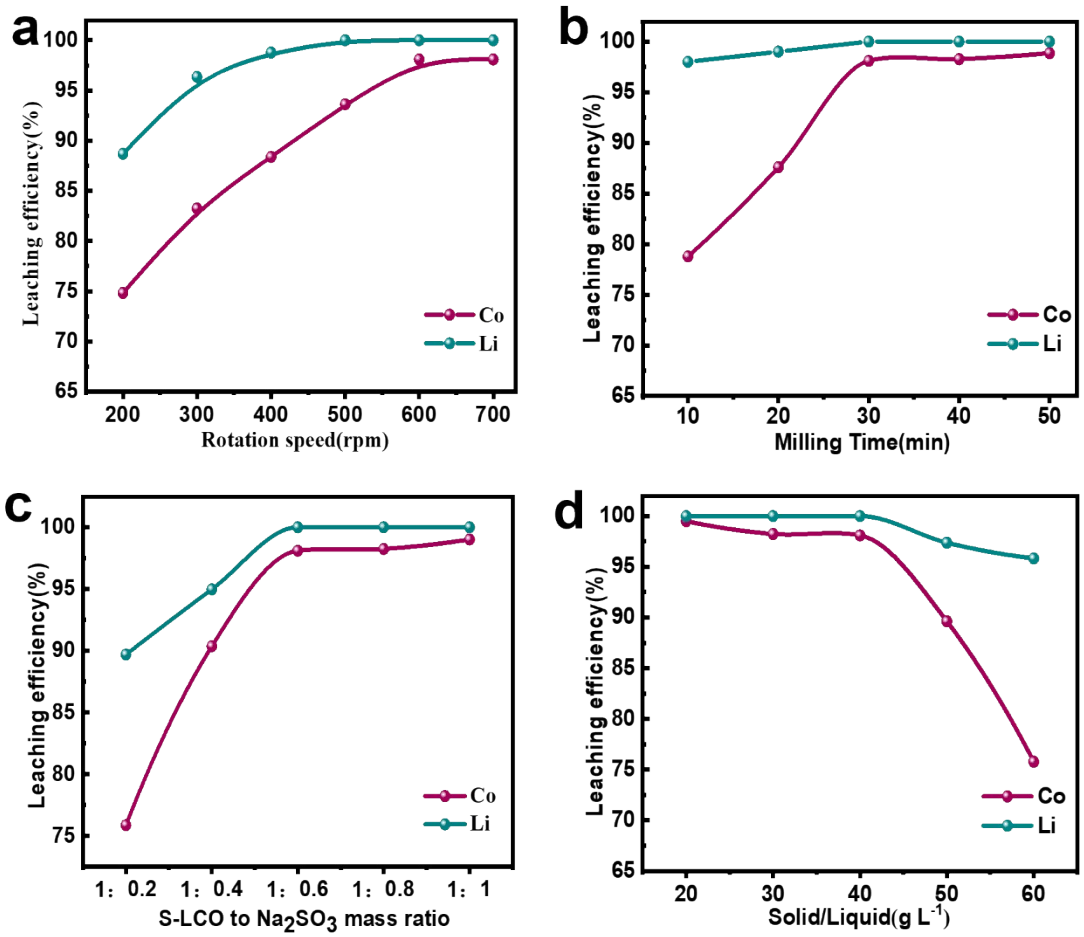

Figure S2. Effect of (a) rotation speed, (b) milling time, (c) mass ratio and (d) solid/liquid on the leaching efficiencies of valuable metals in S-LCO/Na_2SO_3 powders.

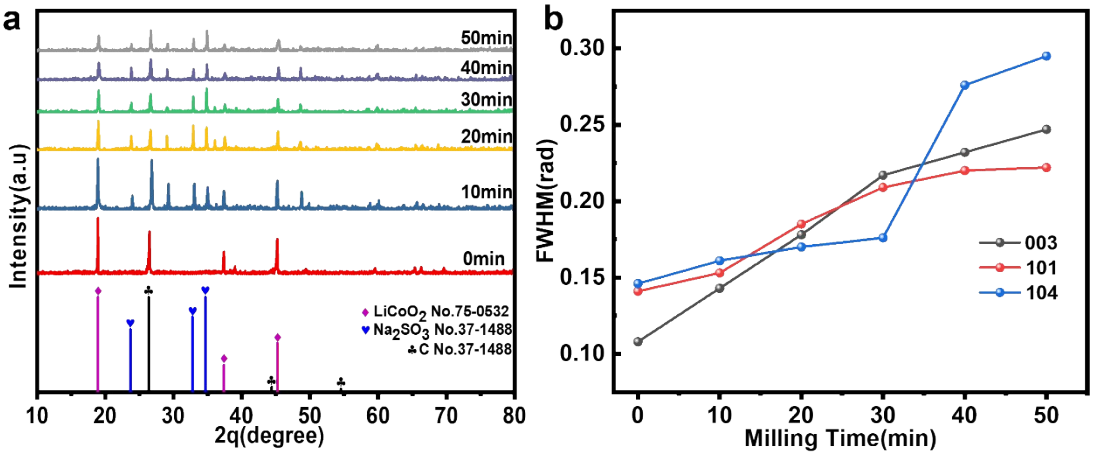

Figure S3. (a) XRD patterns, (b) FWHM of S-LCO/Na_2SO_3 powders activated at 600 rpm for different milling times.

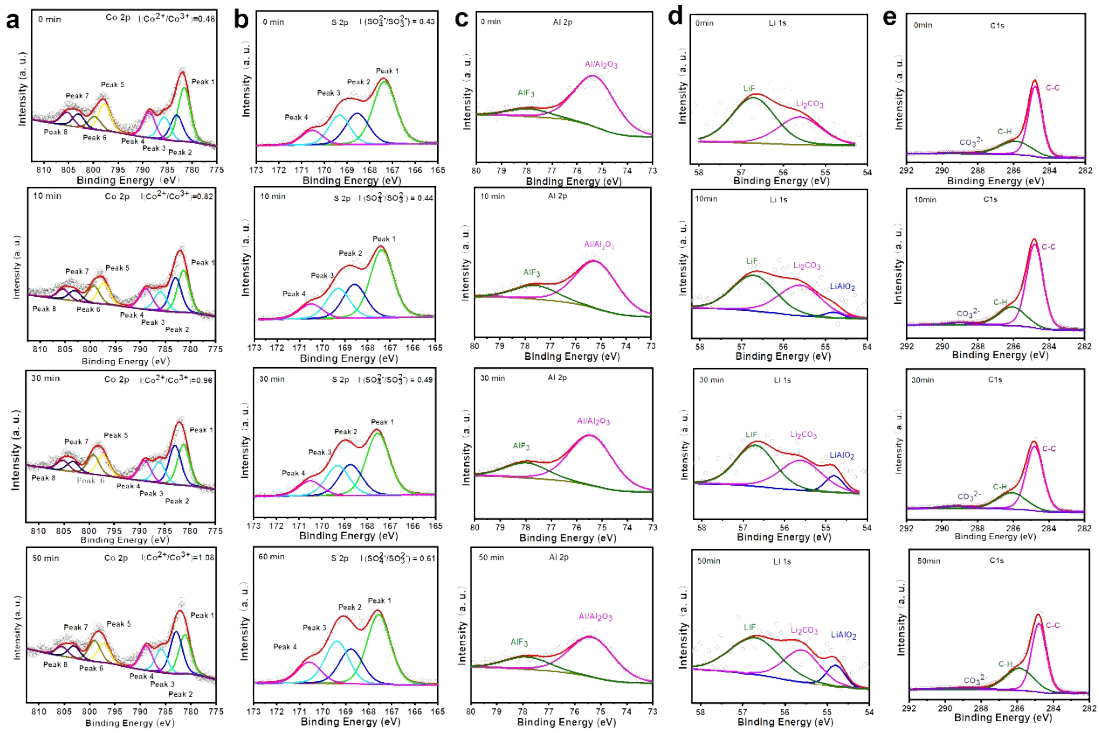

Figure S4. High-resolution XPS spectra of (a) Co 2p, (b) S 2p, (c) Al 2p, (d) Li 1s and (e) C 1s of the S-LCO/Na_2SO_3 (mass ratio of 1:0.6) powders activated at 600 rpm for different milling times.

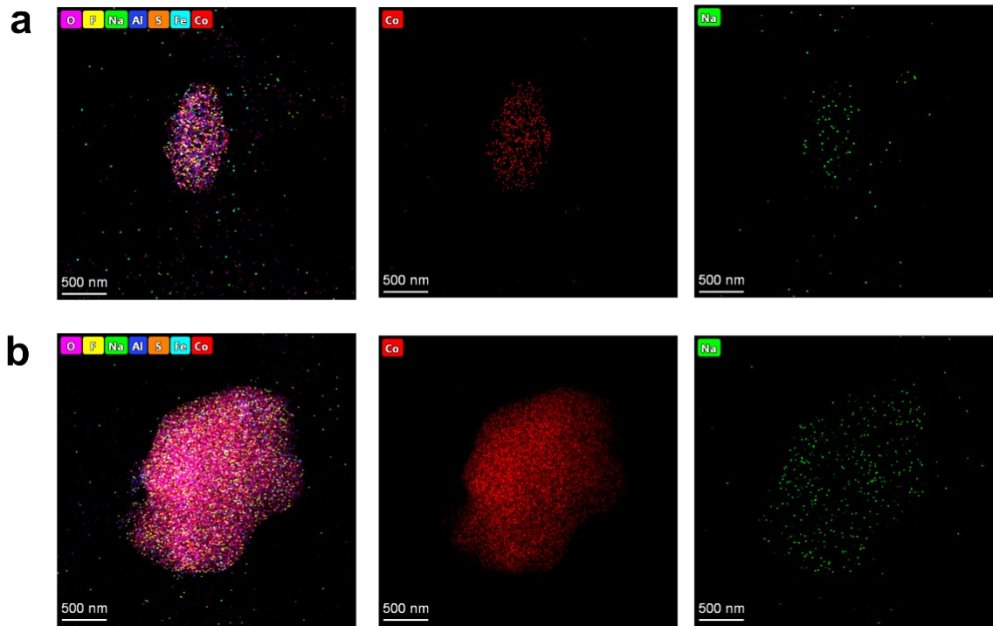

Figure S5. EDS mapping of elements Co and Na of the S-LCO/Na_2SO_3 (mass ratio of 1:0.6) powders before activation (0 min) and after activated at 600 rpm for 30 min.

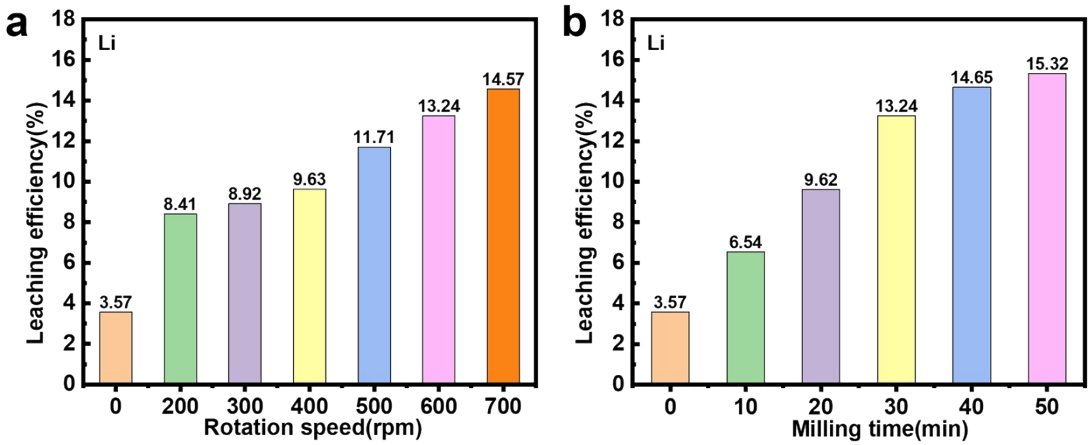

Figure S6. The leaching efficiency of Li in water from S-LCO/Na_2SO_3 powders under different activation conditions: (a) milling 30 min at different rotation speeds, (b) milling different times at 600 rpm (Leaching conditions: after the mechanochemical reaction, using deionized water as the leaching agent, Li^+ was directly leached at room temperature with a solid-liquid ratio of 40 g L^{-1}).

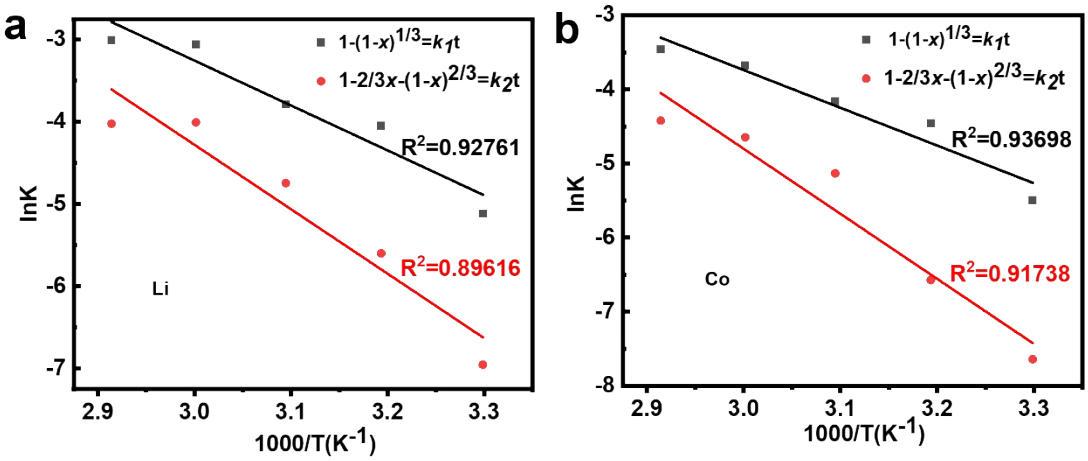

Figure S7. Arrhenius plots for leaching of (a) Li and (b) Co from the S-LCO/Na_2SO_3 powders activated at 600 rpm for 30 min.

Table S1. Fitting peaks of XPS spectra for the Co 2p of S-LCO/Na_2SO_3 powders activated at 600 rpm for different milling times.

		Co $2p_{3/2}$				Co $2p_{1/2}$				$I(Co^{2+}/Co^{3+})$
		Peak1 Co^{3+}	Peak2 Co^{2+}	Peak3 Co^{2+} Sat	Peak4 Co^{3+} Sat	Peak5 Co^{3+}	Peak6 Co^{2+}	Peak7 Co^{2+} Sat	Peak8 Co^{3+} Sat	
0	Position(eV)	781.60	783.11	785.61	788.65	797.70	799.71	802.99	805.33	0.48
	Aera (%)	27.74	13.45	11.48	13.19	13.87	6.72	6.59	6.93	
10min	Position(eV)	781.40	782.97	785.96	788.86	797.3	799.29	803.09	805.41	0.83
	Aera (%)	23.44	19.84	11.88	12.73	12.07	9.92	6.36	6.03	
30min	Position(eV)	781.31	782.98	786.09	788.97	797.24	799.15	803.16	805.18	0.96
	Aera (%)	22.42	21.54	11.49	11.29	11.21	10.77	5.64	5.60	
50min	Position(eV)	781.20	782.90	785.83	788.81	797.23	799.03	803.09	805.47	1.08
	Aera (%)	20.36	22.06	12.03	12.82	10.18	11.03	6.41	5.09	

The data of the fitting peaks of the Co 2p XPS spectra was calculated by the XPS peak software.

Content of Co^{2+} = $(Aera_{peak2} + Aera_{peak6})/(Aera_{peak1} + Aera_{peak2} + Aera_{peak5} + Aera_{peak6})$

Content of Co^{3+} = $(Aera_{peak1} + Aera_{peak5})/(Aera_{peak1} + Aera_{peak2} + Aera_{peak5} + Aera_{peak6})$

$I(Co^{2+}/Co^{3+})$ = Content of Co^{2+}/Content of Co^{3+}

Table S2. Fitting peaks of XPS spectra for the S 2p of S-LCO/Na_2SO_3 powders activated at 600 rpm for different milling times.

		S $2p_{3/2}$		S $2p_{1/2}$		$I(SO_4^{2-}/SO_3^{2-})$
		Peak1 SO_3^{2-}	Peak3 SO_4^{2-}	Peak2 SO_3^{2-}	Peak4 SO_4^{2-}	
0	Position(eV)	167.35	169.32	168.55	170.52	0.43
	Aera (%)	46.50	20.16	23.25	10.08	
10min	Position(eV)	167.37	169.29	168.57	170.49	0.44
	Aera (%)	46.20	20.46	23.10	10.23	
30min	Position(eV)	167.54	169.30	168.74	170.50	0.49
	Aera (%)	44.82	21.85	22.41	10.92	
50min	Position(eV)	167.57	169.38	168.77	170.58	0.61
	Aera (%)	41.41	25.26	20.70	12.63	

The data of the fitting peaks of the S 2p XPS spectra was calculated by the XPS peak software.

Content of SO_3^{2-} = $(Aera_{peak1} + Aera_{peak2})/(Aera_{peak1} + Aera_{peak2} + Aera_{peak3} + Aera_{peak4})$

Content of SO_4^{2-} = $(Aera_{peak3} + Aera_{peak4})/(Aera_{peak1} + Aera_{peak2} + Aera_{peak3} + Aera_{peak4})$

$I(SO_4^{2-}/SO_3^{2-})$ = Content of SO_4^{2-}/Content of SO_3^{2-}

Table S3. Fitting peaks of XPS spectra for the Al 2p of S-LCO/Na_2SO_3 powders activated at 600 rpm for different milling times.

		Al/Al_2O_3	AlF_3
		Peak1	Peak2
0	Position(eV)	75.29	77.89
	Aera (%)	86.73	13.27
10min	Position(eV)	75.16	77.57
	Aera (%)	77.50	22.50
30min	Position(eV)	75.42	77.97
	Aera (%)	76.77	23.23
50min	Position(eV)	75.34	77.84
	Aera (%)	76.17	23.83

Table S4. Fitting peaks of XPS spectra for the C 1S of S-LCO/Na_2SO_3 powders activated at 600 rpm for different milling times.

		C-C	C-H	CO_3^{2-}
		Peak1	Peak2	Peak3
0	Position(eV)	284.80	285.90	289.15
	Aera (%)	67.26	29.97	2.77
10min	Position(eV)	284.80	286.07	289.01
	Aera (%)	70.89	25.90	3.21
30min	Position(eV)	284.80	286.08	289.21
	Aera (%)	66.68	29.07	4.25
50min	Position(eV)	284.80	285.88	289.02
	Aera (%)	57.68	36.23	6.09

Table S5. The rate constant (k) and the coefficient of determination (R^2) for Li and Co leaching from the S-LCO/Na_2SO_3 powders activated at 600 rpm (30 min) for different temperatures**.**

Model	Equation	T(k)	Li		Co		Ea (kJ mol^{-1})	
			k (min^{-1})	R^2	k (min^{-1})	R^2	Li	Co
Chemical reaction control	$1 - (1-x)^{\frac{1}{3}} = k_1 t$	303.15	0.0060	0.9844	0.0041	0.9941	45.40	42.32
		313.15	0.0175	0.9950	0.0116	0.9929		
		323.15	0.0227	0.9927	0.0156	0.9919		
		333.15	0.0470	0.9926	0.0253	0.9955		
		343.15	0.0494	0.9888	0.0314	0.9925		
Internal diffusion control	$1 - \frac{2}{3}x - (1-x)^{2/3}$	303.15	9.5626E-4	0.9889	4.8076E-4	0.9979	65.15	72.95
		313.15	0.0037	0.9973	0.0014	0.9831		
		323.15	0.0087	0.9846	0.0059	0.9804		
		333.15	0.0182	0.9670	0.0096	0.9721		
		343.15	0.0179	0.9698	0.0120	0.9817		

Table S6. Test liquids and their surface tension[1–3]

Liquids	Total surface tension (mN/m)	Dispersive component (mN/m)	Polar component (mN/m)
deionized water	72.8	21.8	51.0
n-hexadecane	27.6	27.6	0.0

According to the Owens−Wendt−Rabel−Kaelble (OWRK) method, the interfacial tension of each phase can be divided into two parts: a polar component, γ^p, and a non-polar component (dispersion component), γ^d. The surface free energy between the solids and liquids is γ_{sl}. The relationship between γ_{sl}, γ^p and γ^d can be expressed by OWRK as follows:

$$\gamma_{sl} = \gamma_l + \gamma_s - 2\left(\gamma_l^d \gamma_s^d\right)^{1/2} - 2(\gamma_l^p \gamma_s^p)^{1/2} \quad \textbf{(Eq. S1)}$$

According to Young's equation (**Eq. S2**), the relationship between the contact angle of a liquid on a solid surface (θ) and the free energy between solid, liquid and gas can be expressed as:

$$\cos\theta = (\gamma_s - \gamma_{sl})/\gamma_l \quad \textbf{(Eq. S2)}$$

where γ_l, γ_s and γ_{sl}, are the surface free energy of liquids, the surface free energy of solids, and the free energy at the solid–liquid interface, respectively. Substituting **Eq. S1** into **Eq. S2** gives:

$$\gamma_l(1 + \cos\theta) = 2\left(\gamma_l^d \gamma_s^d\right)^{1/2} + 2(\gamma_l^p \gamma_s^p)^{1/2} \quad \textbf{(Eq. S3)}$$

$$\frac{\gamma_l(1 + \cos\theta)}{2\sqrt{\gamma_l^d}} = \sqrt{\gamma_s^p} \cdot \sqrt{\frac{\gamma_l^p}{\gamma_l^d}} + \sqrt{\gamma_s^d} \quad \textbf{(Eq. S4)}$$

According to **Eq. S4**, using the data from Table S6, by plotting $\frac{\gamma_l(1 + \cos\theta)}{2\sqrt{\gamma_l^d}}$ versus $\sqrt{\frac{\gamma_l^p}{\gamma_l^d}}$, γ_s^p and γ_s^d can be calculated from the slope and the intercept of the fitted line, respectively. The value of can be determined as a sum of the two surface free energy components (**Eq. S5**).

$$\gamma_s = \gamma_s^p + \gamma_s^d \quad \textbf{(Eq. S5)}$$

Table S7. Summary of leaching parameters for leaching S-LCO in different references.

Leaching agent	Leaching condition				Leaching efficiency		Ref.
	Concentration (mol L^{-1})	Temperature (°C)	Time (min)	Solid-liquid ratio (g L^{-1})	Li (%)	Co (%)	
H_2SO_4	0.5	60	30	40	99.9	98.95	**This work**
H_2SO_4	2	80	240	35	92	88	49
H_2SO_4	2	60	120	33	87.5	96.3	50
H_2SO_4	3	95	120	25	96	98	51
H_2SO_4	1	95	240	20	96.7	91.6	52
HCl	4	80	120	30	97	99	53
HCl	4	80	120	20	99	99	54
HNO_3	1	75	30	20	95	95	55

References [4–8]

[1] D. H. Kaelble, *J. Adhesion*, 1970, **2**, 66.

[2] Y. Gao, R. Guo, R. Fan, Z. Liu, W. Kong, P. Zhang, F.-P. Du, *Pest Manag. Sci.*, 2018, **74**, 1804.

[3] Y. X. Zhuang, O. Hansen, *Langmuir*, 2009, **25**, 5437.

[4] L. Kong, Z. Li, W. Zhu, C. R. Ratwani, N. Fernando, S. Karunarathne, A. M. Abdelkader, A. R. Kamali, Z. Shi, *J. Colloid Interf. Sci.*, 2023, **640**, 1080.

[5] Y. C. Yin, C. Li, X. Hu, D. Zuo, L. Yang, L. Zhou, J. Yang, J. Wan, *ACS Energy Lett.*, 2023, **8**, 3005.

[6] H. Yang, B. Deng, X. Jing, W. Li, D. Wang, *Waste Manage.*, 2021, **129**, 85.

[7] X. Mu, K. Huang, G. Zhu, Y. Li, C. Liu, X. Hui, M. Sui, P. Yan, *Nano Energy*, 2023, **112**, 108465.

[8] K. Lahtinen, E. L. Rautama, H. Jiang, S. Räsänen, T. Kallio, *ChemSusChem*, 2021, **14**, 2434.